

Mechanical properties and microstructures of machinable silicon carbide

KATSUAKI SUGANUMA, GENN SASAKI, TERUAKI FUJITA

Department of Materials Science and Engineering, National Defense Academy, Yokosuka, Kanagawa 239, Japan

MASATOSHI OKUMURA

Nippon-Soda Co. Ltd, Odawara, Kanagawa 250-02, Japan

KOUICHI NIIHARA

Institute of Scientific and Industrial Research, Osaka University, Mihogaoka, Osaka 567, Japan

Mechanical properties and microstructures of machinable silicon carbide, fabricated by pressureless sintering of silicon carbide fine powder with the aid of polysilastyrene, have been examined. Drastic changes in microstructure and in mechanical properties between specimens sintered at below 1773 K and at above 1873 K were observed. By sintering at above 1883 K the machinable silicon carbide had a good strength of more than 200 MPa with high reliability, which was maintained beyond 1773 K. Polysilastyrene was converted into β -phase silicon carbide and ribbon carbon (or graphite) by sintering. The machinable silicon carbide had a porous silicon carbide skeleton with fine ribbon carbon in the pores. The (001) plane of carbon is parallel to the (111) planes of β -phase silicon carbide.

1. Introduction

Machinable ceramics, which can be machine-worked by conventional steel tools, have been recognized as useful ceramic materials. This type of ceramic has the benefit of being formed into a certain component without hard working by diamond tools. Several types of machinable ceramic are commercially available today: h.c.p. phase boron nitride, mica-based ceramics, aluminium nitride based ceramics and silicon nitride–boron nitride composite are typical examples [1]. Silicon carbide based ceramic has also been known as one of the machinable ceramics [2]. It is fabricated by sintering silicon carbide fine powders with polysilastyrene as a binder in an inert atmosphere. Polysilastyrene is known as one of the inorganic polymers that can be converted into silicon carbide by firing [3]. Machinable silicon carbide has quite excellent strength from room temperature to 1773 K. Such good strength up to elevated temperature is one of the main characteristics of silicon carbide. This is one of the benefits by which machinable silicon carbide is distinguished from the other kinds of machinable ceramic, all of which have a maximum operating temperature of about 1300 K.

The aims of the present work were to evaluate the details of the mechanical properties and microstructures of silicon carbide machinable ceramic, in order to understand the origins of the machinability of this ceramic.

2. Experimental procedure

2.1. Materials

β -phase silicon carbide powder (Ibiden, UF grade, 0.3 μm in size) was mixed with 20 wt% of polysilastyrene with a small amount of organic binder. The mixture was injection-moulded into 4 mm \times 3 mm \times 55 mm bars and they were pressureless-sintered 1473–2173 K for 1 h in argon flow. Polysilastyrene was also sintered under the same conditions as those for the machinable ceramic, to examine the products from polysilastyrene. Details of the fabrication process of machinable silicon carbide have been reported in previous work [2].

2.2. Evaluation

The sintered bars were used for density measurement, bending tests and Young's modulus evaluation. Apparent density and average pore size were evaluated by the mercury porosimetric method. Three-point bending strength was measured at room temperature for all specimens. Statistical treatment was carried out by using Weibull statistics and the Weibull modulus was derived by the greatest likelihood method. The sample number was 19. The span for the bending test was 30 mm and the crosshead speed was 0.5 mm min⁻¹. High-temperature strength up to 1773 K was measured for the specimen sintered at

2173 K. Young's modulus was evaluated at room temperature by the vibration resonance method.

Microstructures were examined by scanning electron microscopy (SEM), transmission electron microscopy (TEM) and X-ray diffraction. The transmission electron microscope used was a JEM200CX (Jeol) operated at 200 kV. Sintered bars were crushed into flakes which were then fixed on a carbon grid mesh. Some of the specimens were prepared by conventional argon-ion thinning.

3. Results and discussion

3.1. Effects of sintering temperature on macrostructure

Fig. 1 shows a series of SEM microstructures of machinable silicon carbide sintered at various temperatures. The specimens sintered at 1473 K and at 1773 K show dispersed silicon carbide particles. In the specimen sintered at 1873 K, silicon carbide particles are connected to form certain aggregates and at 2073 K large bridges between silicon carbide particles form the network. Fig. 2 shows an enlarged image of the structure of the specimen sintered at 2073 K. Fine ribbon-like structure of 10 nm scale was recognized which fills pores among silicon carbide particles in Fig. 1.

The changes of apparent density and of average pore size as a function of sintering temperature are shown in Fig. 3. The density was between 2.1 and

2.2 g cm^{-3} and did not change at all up to 2173 K. On the other hand, the average pore size increased gradually with increasing sintering temperature to 1773 K; beyond 1873 K a sharp increase was observed, and above 1973 K the increase tended to terminate. Because the ideal density of silicon carbide is 3.19 g cm^{-3} , the relative density of the machinable silicon carbide is about 66–68%.

3.2. Strength of machinable silicon carbide

Fig. 4 shows the strength and Weibull modulus of the machinable ceramic as a function of sintering temperature. The specimen sintered at below 1773 K had a low strength of about 100 MPa and the Weibull moduli were somewhat small. For sintering above 1873 K, the strength reached 200 MPa and the Weibull modulus increased up to about 15. These distinguishable changes in strength depending on sintering temperature which occurred from 1773 to 1873 K seem to be closely related to the microstructural change observed in Fig. 1. Although below 1773 K silicon carbide particles were distributed discretely and the pores in the skeleton of silicon carbide particles were filled with fine ribbon-like structure, beyond 1873 K silicon carbide particles formed connections with each other. Such formation of skeletons of silicon carbide seems to give the good strength of this ceramic when sintered at above 1873 K.

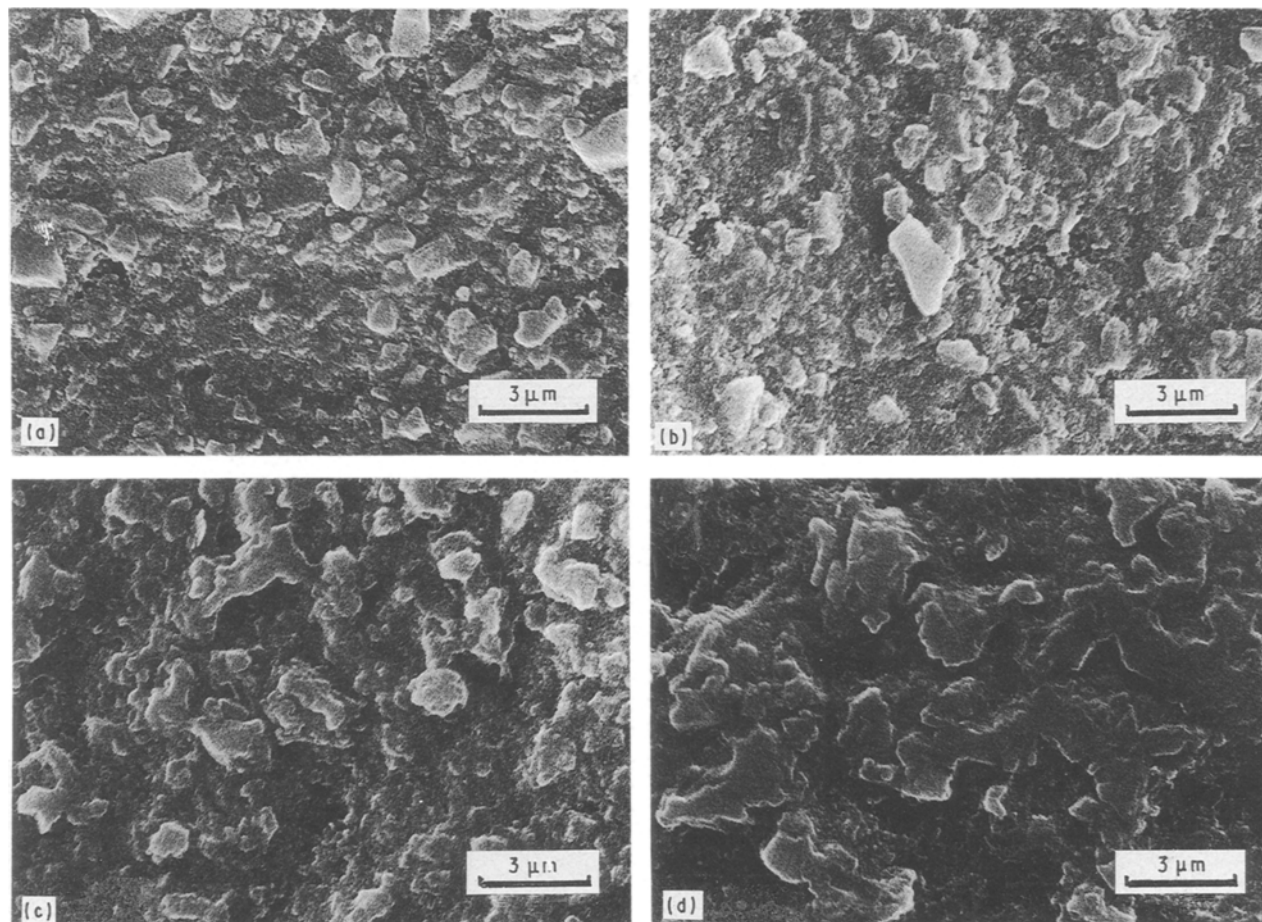


Figure 1 SEM photographs of machinable silicon carbide sintered at (a) 1473 K, (b) 1771 K, (c) 1873 K, (d) 2073 K.

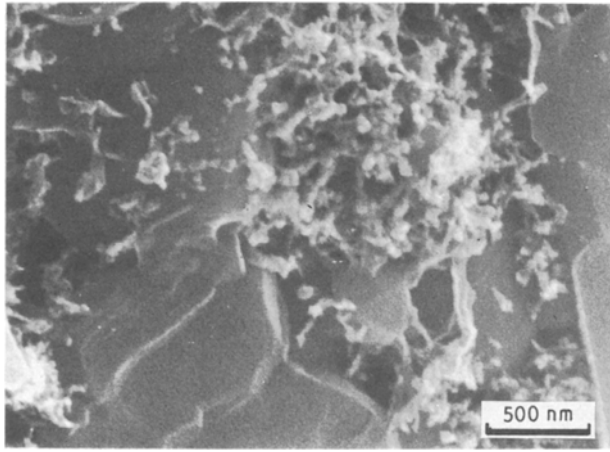


Figure 2 Fracture surface of machinable silicon carbide sintered at 2073 K.

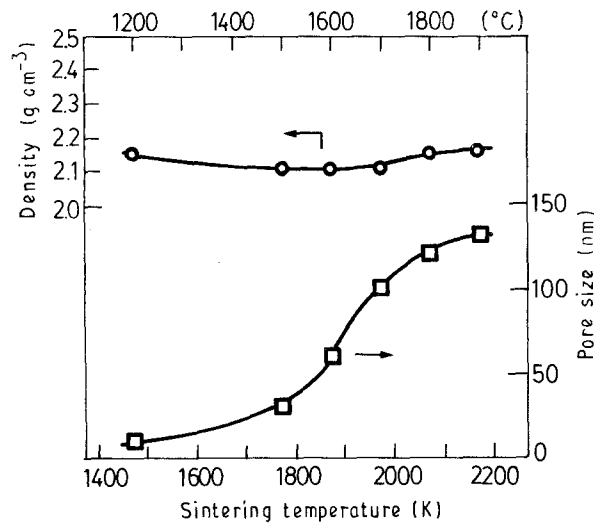


Figure 3 Changes in density and average pore size as a function of sintering temperature of machinable silicon carbide.

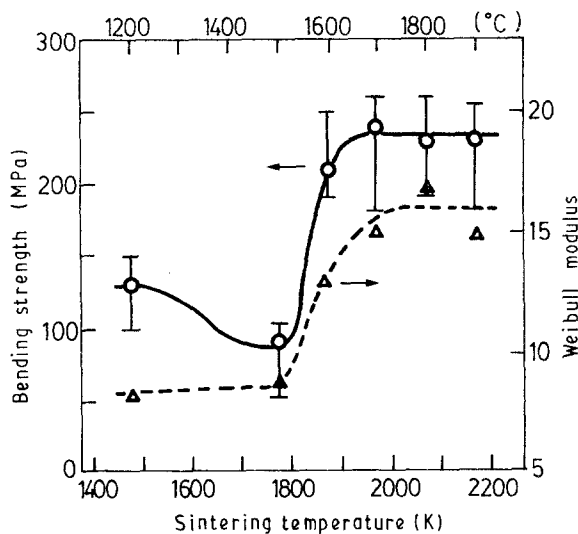


Figure 4 (○) Bending strength and (△) Weibull modulus of machinable silicon carbide as a function of sintering temperature.

Silicon carbide is well known to have heat resistance to over 1800 K. Fig. 5 shows the temperature dependence of strength of the specimen sintered at 2173 K. The strength did not change up to 1673 K and

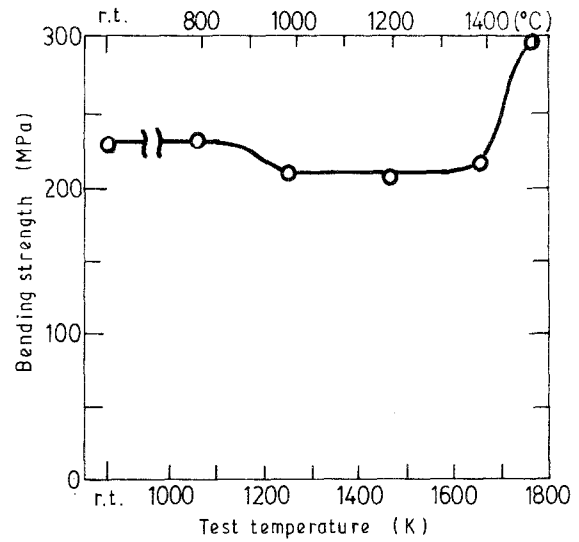


Figure 5 High-temperature bending strength of machinable silicon carbide sintered at 2173 K.

increased slightly at 1773 K, which is the typical tendency of silicon carbide ceramics.

Fig. 6 shows the change in Young's modulus as a function of sintering temperature. The dependence on sintering temperature is almost the same as observed for the strength. From 1773 to 1873 K, Young's modulus increased sharply. This sharp increase also seems to be due to the formation of the skeletons of silicon carbide. However, the values for specimens sintered at above 1873 K were between 100 and 120 GPa, which is not large compared with that of dense silicon carbide (beyond 400 GPa). The low Young's modulus seems to be due to the porous structure of this ceramic.

Other kinds of machinable ceramic such as h.c.p. boron nitride, the mica-based ceramics and so on have a strength level of about 100 MPa. Their heat-resistant temperatures are limited to about 1300 K because of the nature of the sintering binders or the oxidation resistance. Compared with them, machinable silicon carbide has twice as high a strength level and keeps it for a further 500 K. Therefore, it can be

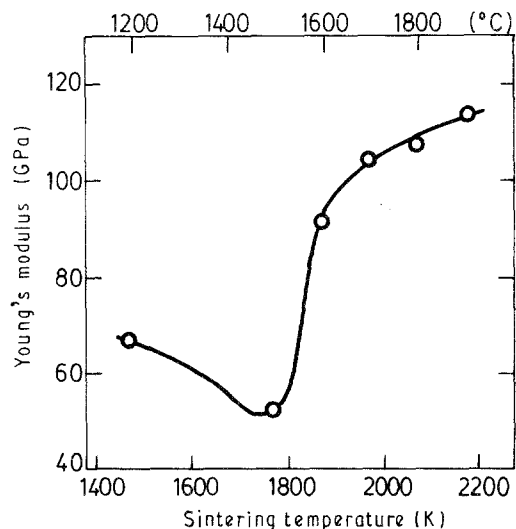


Figure 6 Young's modulus of machinable silicon carbide as a function of sintering temperature.

said that this ceramic is one of the most promising high-temperature structural machinable ceramics.

3.3. Microstructural observation with TEM

Fig. 7 shows a representative microstructure of high strength machinable silicon carbide sintered at 2073 K. Silicon carbide particles connect each other and fine ribbon-like structures fill the pores, which have also been observed in SEM observation (see Fig. 2). Silicon carbide particles are below 1 μm in diameter and, therefore, it is noted that little grain growth occurs during sintering treatment considering the fact that the starting powder is 0.3 μm in grain size.

Polysilastyrene, which was the binder used to sinter silicon carbide, is known to be one of the inorganic polymers converting basically into silicon carbide [4]. To understand the structure of the machinable silicon carbide, it is worthwhile to distinguish the roles of silicon carbide powder and the silicon carbide formed by reaction from polysilastyrene. Therefore, polysilastyrene without silicon carbide powder was sintered under the same conditions and examined. Fig. 8 shows X-ray diffraction patterns taken from three selected specimens. For sintering at 1473 K, broad peaks of β -phase silicon carbide and one sharp peak which corresponds to that of carbon (or graphite) were recognized. Broadening of the silicon carbide peaks in the present case seems to indicate the fine particulate structure of β -phase silicon carbide.

The peak for carbon, which has the lattice distance of 0.34 nm, corresponds to careful observation of the TEM micrograph in Fig. 7 showing that the spacing of the lattice images observed in the ribbon-like structures is about 0.34 nm, as also shown below. Therefore, the ribbon-like structure turns out to be the so-called ribbon carbon. Sintering beyond 1773 K made the peaks of β -phase silicon carbide sharper, and an additional two small peaks in the low-angle region were recognized. The two new peaks seem to be from the long-range ordering of β -phase silicon carbide. With increasing sintering temperature the peak of the carbon became broader towards higher angles than for that sintered at 1473 K. This fact indicates that the

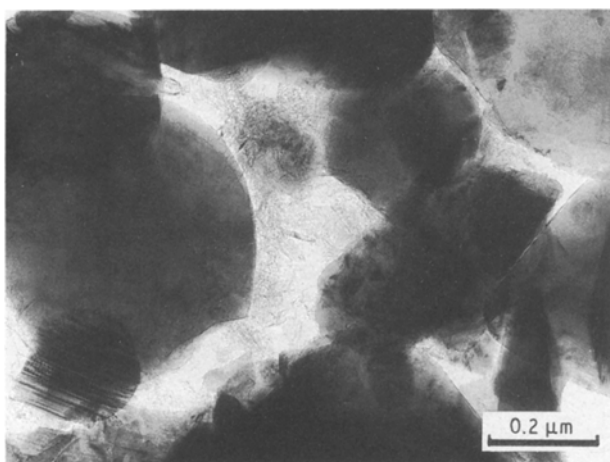


Figure 7 TEM micrograph of machinable silicon carbide sintered at 2073 K.

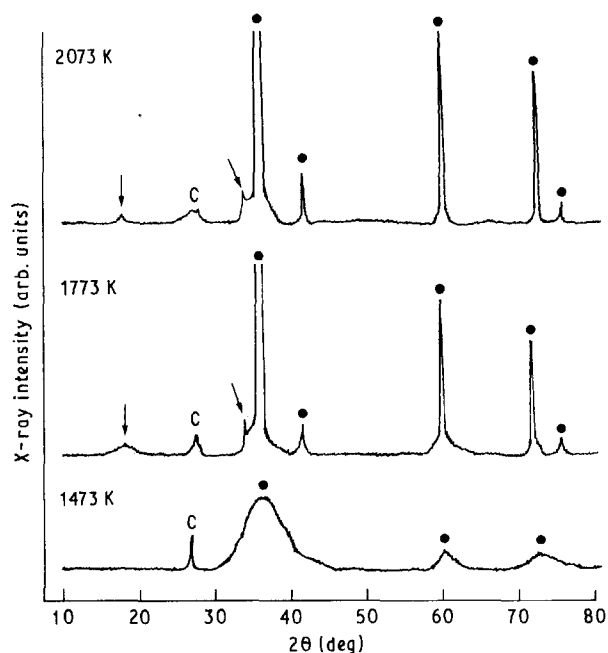


Figure 8 X-ray diffraction patterns from polysilastyrene sintered at 1473, 1773 and 2073 K. The arrows indicate the long-range ordering of β -phase silicon carbide and "C" indicates the (0 0 2) plane of carbon/graphite.

ribbon carbon changed gradually into graphite. Thus, polysilastyrene is turned into β -phase silicon carbide and ribbon carbon under the present sintering conditions.

Fig. 9 shows two typical TEM microstructures of polysilastyrene sintered at 1773 and 2073 K without

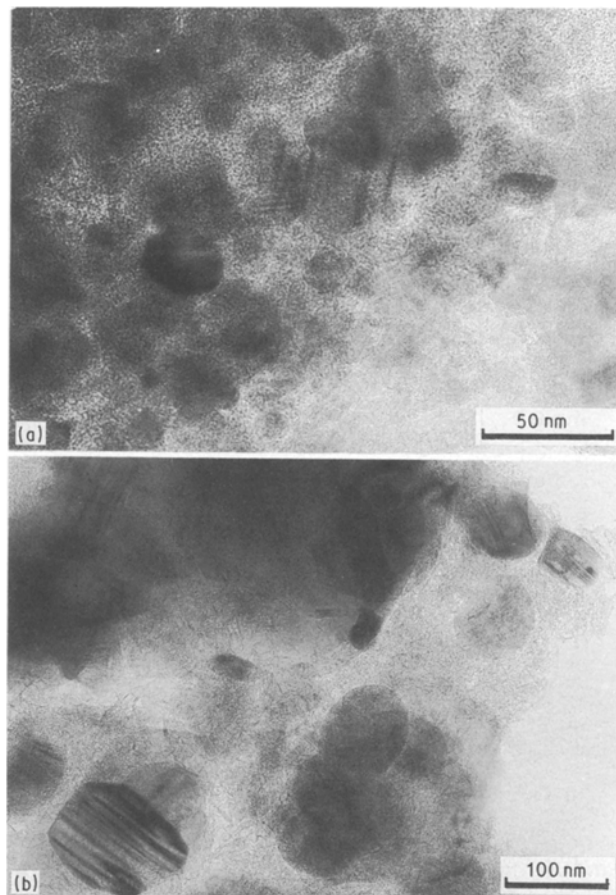


Figure 9 TEM photographs of polysilastyrene sintered at (a) 1773 K and (b) 2073 K.

silicon carbide powder. In both cases, the structure consisted of fine particles and the finer ribbon structure. The particles are β -phase silicon carbide and the ribbon structures are ribbon carbon. When sintered at 1773 K the silicon carbide particles were 10–30 nm in diameter and at 2073 K these grew up to about 100 nm. The ribbon structure sintered at 1773 K is very fine as seen in Fig. 10. The ribbon has two or three layers of the (002) planes of carbon/graphite, 0.34 nm spacing, and, therefore is narrower than 1 nm. In the silicon carbide particles, stacking fault structure is apparent. On increasing the firing temperature, the width of the ribbon carbon became thicker as shown in Fig. 11. It has more than five layers of the (002) planes of carbon.

A certain crystallographic orientation relationship between the β -phase silicon carbide and ribbon carbon is observed in Fig. 11. The basal plane of the carbon is almost parallel to the (111) planes of β -phase silicon carbide, as indicated in Fig. 11. This phenomenon was frequently observed in TEM observation. Fig. 12 shows the surface of a large silicon carbide particle greater than 1 μm in diameter in the machinable silicon carbide. This particle seems to have grown during sintering from one of the silicon carbide

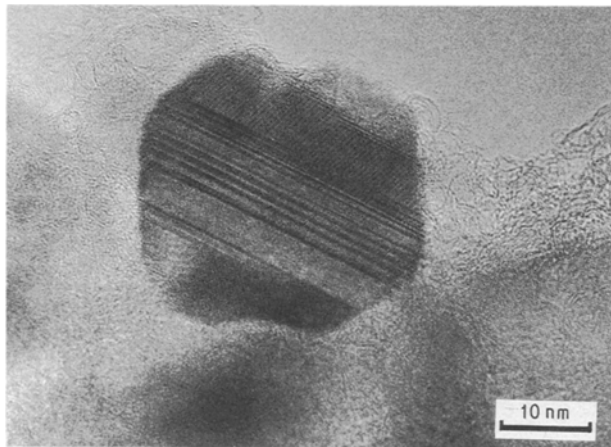


Figure 10 HREM of polysilastyrene sintered at 1773 K. The electron beam is parallel to the [1 1 0] axis of the silicon carbide particle.

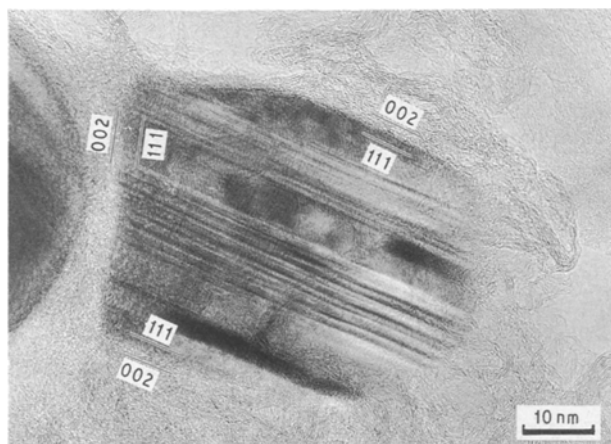


Figure 11 HREM of the polysilastyrene sintered at 2073 K. The electron beam is parallel to the [1 1 0] axis of the silicon carbide particle.

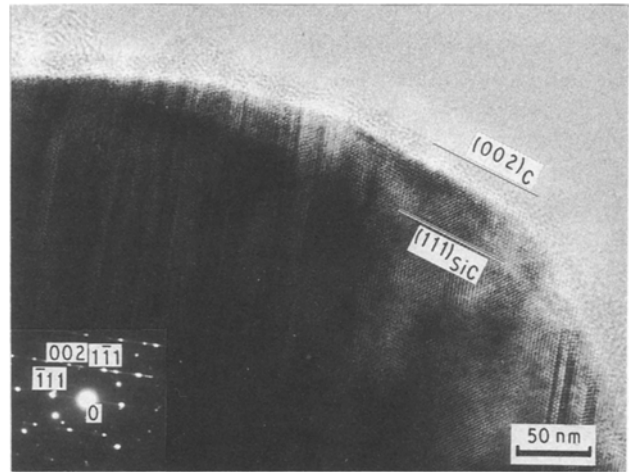


Figure 12 HREM of the surface of a large silicon carbide particle in machinable silicon carbide sintered at 2073 K. The electron beam is parallel to the [1 1 0] axis of the silicon carbide particle.

starting particles. On the (111) plane of the silicon carbide particle alone, the basal plane of the carbon becomes parallel to it and on the others the structure is distorted. This crystallographic relationship is expressed as follows:

$$\{111\}_{\beta\text{-phase silicon carbide}} // \{001\}_{\text{carbon}}$$

The same relationship has been also reported by Yajima and Hirai [4]. In the CVD process, only on the {111} plane of the single crystal of β -phase silicon carbide the (001) planes of graphite grow to form a single crystal. Thus, this crystallographic relationship seem to have the benefit of forming a certain low-energy interface between β -phase silicon carbide and carbon (or graphite).

Fig. 13 shows the TEM microstructure of ion-thinned machinable silicon carbide sintered at 2073 K. The ribbon carbon structure was damaged by ion-thinning and it became an amorphous structure. It is clearly observed that the silicon carbide grains are connected to each other to form tight boundaries and

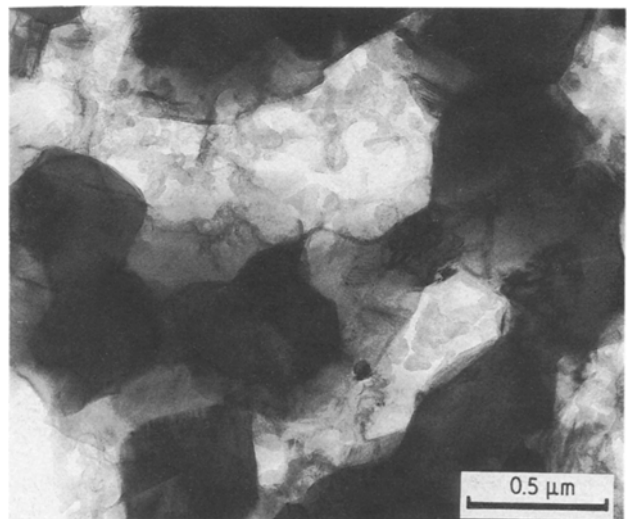


Figure 13 TEM photograph of ion-thinned machinable silicon carbide. The ribbon carbon became amorphous due to damage during thinning.

the grain sizes are below 1 μm in most cases. These two facts seem to give the ceramic a high strength even though this ceramic has a large porosity.

The reaction-formed carbon was sometimes enclosed in the silicon carbide matrix as particles, as shown in Fig. 14. The particles were below 100 nm in diameter. In the particle the (001) plane of carbon (or graphite) is also parallel to the (111) plane of the β -phase silicon carbide and the particle has a flat interface of the (111) planes of the matrix.

3.4. Mechanism of machinability

There is at present no definition to determine the machinability of ceramics. To show the machinability of the present silicon carbide ceramics, the same sil-

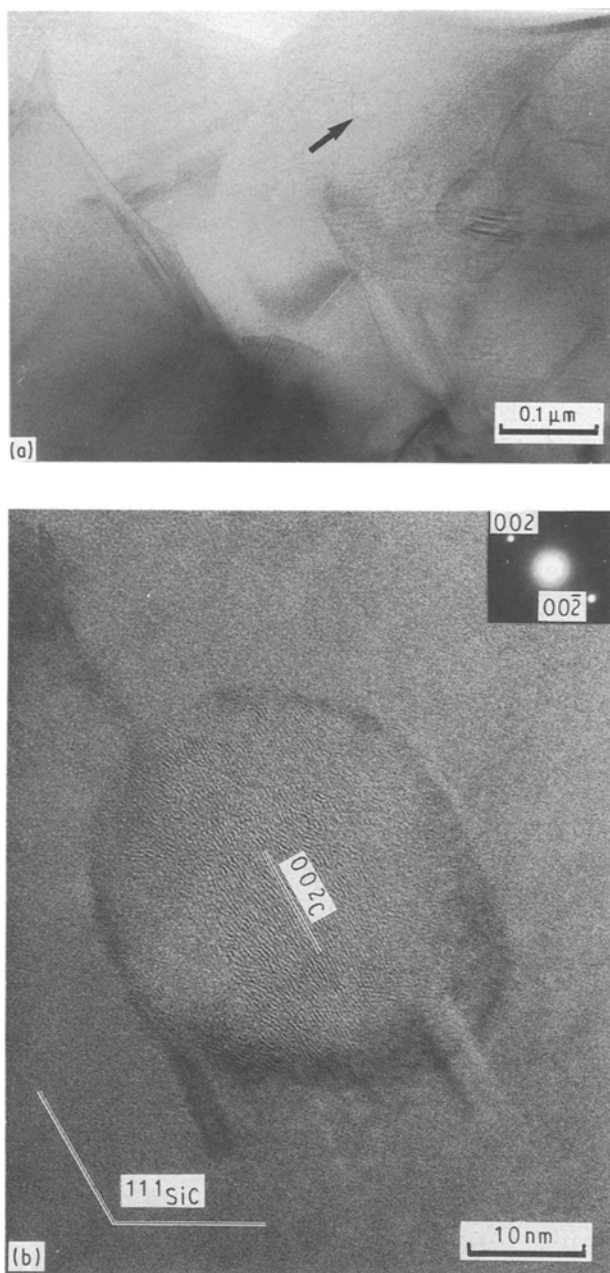


Figure 14 (a) Microstructure in the silicon carbide matrix of machinable silicon carbide. The arrow indicates a small particle in the matrix. (b) HRTEM of the arrowed particle in (a). The incident beam was slightly inclined from the [1 1 0] axis of the matrix. A faint contrast of stacking faults on the (1 1 1) plane in the matrix is recognized.

icon carbide powder without polysilastyrene was sintered at 2173 K for 1 h under a pressure of 30 MPa in 1 atm argon atmosphere by hot-pressing and was compared for machinability. The hot-pressed silicon carbide had a density of 2.0 g cm^{-3} which was almost the same as that of machinable silicon carbide. The average bending strength of the hot-pressed silicon carbide was 140 MPa, which was 100 MPa lower than that of the machinable silicon carbide. 3 mm thick plates were cut from the specimen, and were cut 4 mm in depth from one of the edges by a saw made of low-alloy steel at a constant speed under an applied load of 1.1 N. Fig. 15 shows SEM photographs of the edges of two blades after cutting the two silicon carbides. It became clear that cutting the hot-pressed silicon carbide wore the blade severely but that cutting the machinable silicon carbide ceramic did not. As silicon carbide is well-known as one of the abrasive powders, the severe abrasive wear seen in cutting the hot-pressed silicon carbide is expected. Even though the density was almost the same in both silicon carbides, the machinability of the present silicon carbide was quite excellent. The origin of the machinability of this silicon carbide is considered to lie in the presence of carbon in the pores, and it covers all surfaces of silicon carbide as shown in Fig. 12. Because carbon has good lubricity, it prevents severe wear of the steel blade during cutting.

As shown in the present work, the machinable silicon carbide has the uncommon structure of a mixture of porous silicon carbide skeletons with fine ribbon carbon in the pores. Such a structure gives the ceramic good strength with excellent machinability. Fig. 16 shows an example of the products made using this ceramic. The picture shows a silicon carbide pipe with a threaded end. In conclusion, this silicon carbide would be an excellent structural material having good machinability as well as good strength and heat resistance beyond 1773 K.

4. Conclusion

In the present work the mechanical properties and microstructure of machinable silicon carbide, fabricated by pressureless sintering of silicon carbide fine powder with the aid of polysilastyrene, have been examined. The following results were obtained.

1. There is a drastic change in microstructure and mechanical properties between sintering at below 1773 K and at above 1873 K. By sintering at above 1883 K the machinable silicon carbide has a good strength of more than 200 MPa with high reliability.
2. The machinable silicon carbide maintains a good strength beyond 1773 K.
3. Polysilastyrene is converted into β -phase silicon carbide and ribbon carbon by sintering. The machinable silicon carbide has porous silicon carbide skeletons with fine ribbon carbon in the pores.

4. There exists a crystallographic orientation relationship between β -phase silicon carbide and carbon as follows:

$$\{111\}_{\beta\text{-phase silicon carbide}} // \{001\}_{\text{carbon}}$$

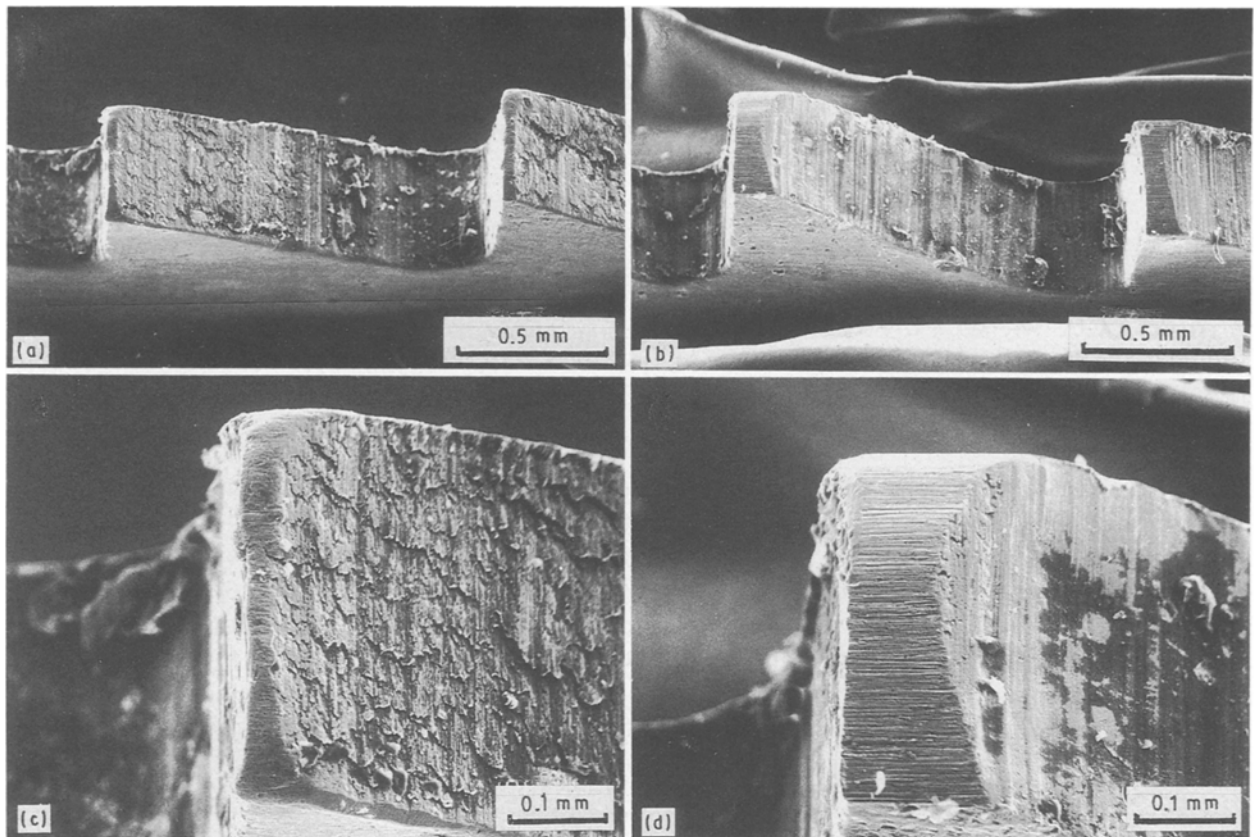


Figure 15 SEM photographs of a steel saw after cutting two silicon carbides: (a, c) silicon carbide sintered at 2173 K by hot-pressing without polysilastyrene; (b, d) machinable silicon carbide sintered at 2073 K.

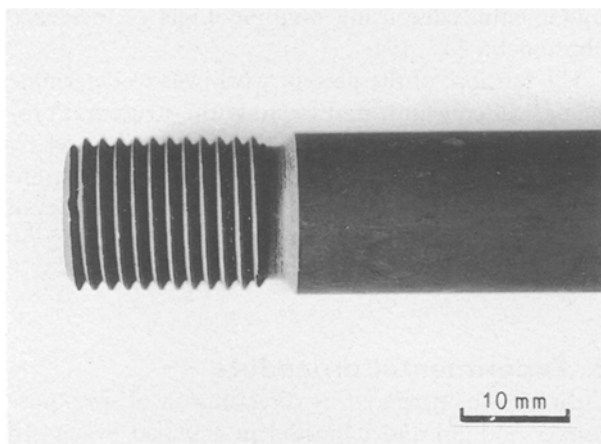


Figure 16 A threaded pipe made from machinable silicon carbide.

The present work has been focused on machinable silicon carbide and discussed the relationship between the mechanical properties/microstructures and the machinability. The presence of lubricant carbon filling

the pores in the hard skeletons has turned out to be one of the key structures for machinability. This structure is not only available for the silicon carbide but is also expected to be adopted by other kinds of ceramic to give the machinability. This structure is considered to be one of the universal structures for machinable ceramics.

References

1. A. MAKISHIMA, A. ASAMI and Y. OGURA, *J. Amer. Ceram. Soc.* **72** (1989) 1024.
2. K. NIIHARA, T. YAMAMOTO, R. TAKEMOTO, K. SUGANUMA and M. OKUMURA, in "Ultrastructure Processing of Advanced Ceramics" edited by J. D. Mackenzie and D. R. Ulrich (Wiley, New York, 1988) p. 547.
3. R. WEST, *Amer. Ceram. Soc. Bull.* **62** (1983) 899.
4. S. YAJIMA and T. HIRAI, *J. Mater. Sci.* **4** (1969) 424.

Received 2 September 1991
and accepted 24 July 1992